

A large gap opening of graphene induced by the adsorption of CO on the Al-doped site

Ali Ahmadi Peyghan · Maziar Noei ·
Mohammad Bigdeli Tabar

Received: 19 December 2012 / Accepted: 19 March 2013 / Published online: 7 April 2013
© Springer-Verlag Berlin Heidelberg 2013

Abstract We investigated CO adsorption on the pristine, Stone-Wales (SW) defected, Al- and Si- doped graphenes by using density functional calculations in terms of geometric, energetic and electronic properties. It was found that CO molecule is weakly adsorbed on the pristine and SW defected graphenes and their electronic properties were slightly changed. The Al- and Si- doped graphenes show high reactivity toward CO, so calculated adsorption energies are about -11.40 and -13.75 kcal mol $^{-1}$ in the most favorable states. It was found that, among all the structures, the electronic properties of Al-doped graphene are strongly sensitive to the presence of CO molecule. We demonstrate the existence of a large E_g opening of 0.87 eV in graphene which is induced by Al-doping and CO adsorption.

Keywords Bandgap · DFT · Graphene · Sensor

Introduction

As a toxic gas, carbon monoxide (CO) still remains one of the major gaseous pollutants associated with automotive emissions, combustion or natural gas manufacturing, industrial activities as well as numerous fires. The threshold limited value for CO is about 3–5 ppm. When the concentration of

CO is higher than 15 ppm it is dangerous for the human body [1]. Consequently, reliable, low-cost CO sensors with high sensitivity and selectivity at low temperatures, and low energy consumption have been required for environmental safety and industrial control. Many sensors have been developed so far for different applications to monitor CO with acceptable level of accuracy [2–7].

Since their discovery in experiments in 2004 [8], graphene and graphene-like materials have been under investigation theoretically and experimentally because of their novel physical and chemical properties [9–11]. Due to their unique structure and properties, these new materials show great potential in many fields, particularly in the field of nanodevices, such as chemical sensors [12–14]. Studies of as-grown graphene, radiation treated graphite and other carbon nanostructures have revealed that defects are common phenomena in carbon-based nanomaterials. Therefore, understanding the properties of intrinsic or artificial defects has become essential for the further development of many applications such as nanoelectronic devices, intramolecular junction and graphene-based lithium batteries. It is well known that pristine graphene is a zero-gap semimetal, and it always has zero energy finite conductivity, which prevents pinch off of the field effect transistor, so pristine graphene cannot provide an on-off signal ratio [15] which is an essential feature of traditional semiconductors. Thus, opening and tuning the bandgap of graphene are especially crucial to its practical application in electronic devices. Recently, several schemes have been proposed to open and tune the bandgap of graphene such as graphene-substrate interaction [16], patterned hydrogen adsorption [17], controlled adatom deposition [18] physical cutting single-layer graphene into nanoribbons [19] or etching it into antidot lattices [20].

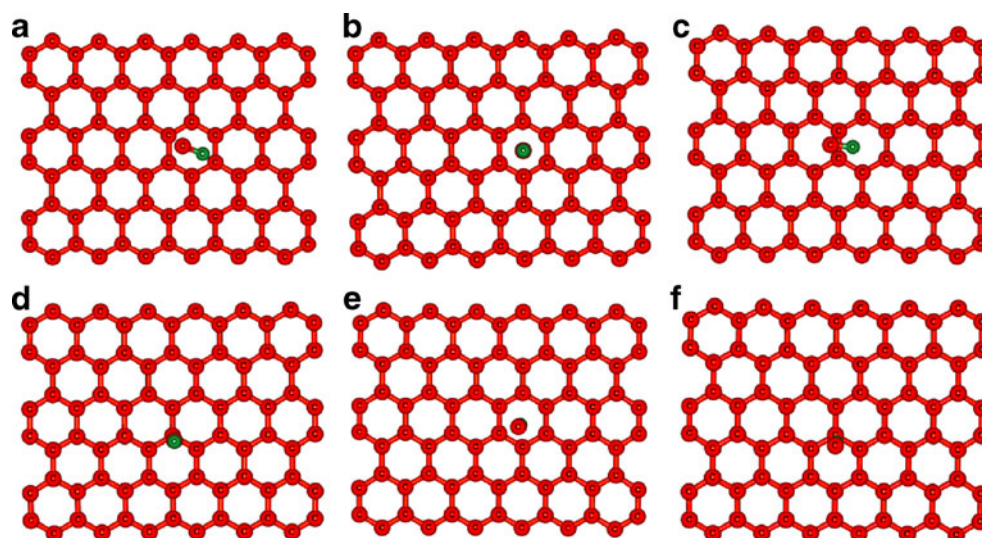
After its successful fabrication, experiments have shown that graphene can be a good sensor for gases such as NO $_2$ and NH $_3$ with high sensitivity [12–14]. Basically, it is expected

A. A. Peyghan
Young Researchers and Elite club, Central Tehran Branch, Islamic Azad University, Tehran, Iran

M. Noei (✉)
Department of Chemistry, Mahshahr Branch, Islamic Azad University, Mahshahr, Iran
e-mail: noeimaziar@gmail.com

M. B. Tabar
Physics group, Science department, Islamic Azad University, Islamshahr Branch, Islamshahr, P.O. Box: 33135-369, Tehran, Iran

Fig. 1 Model for different stable adsorption of CO on the P-graphene. Bonds are in Å



that the adsorption of gas molecules on sensors is stable and changes of the conductivity should be observable. However, most gases are found physisorbed on suspended pristine graphene (P-graphene) [21]. On the contrary, the dopants and defects in graphene may enhance the adsorption of molecules [21], indicating that doped atoms and defects play important roles in the applications of them. In the present work, within the density functional theory (DFT) framework, the interaction of CO with graphene will be investigated based on analyses of structure, energies, electronic properties, etc. We are interested in whether there is a potential possibility of graphene serving as a chemical sensor to CO molecule, and if not, can we find a method for improving the sensitivity of graphene to CO?

Computational methods

We selected a graphene that consisted of 78 C atoms, in which the end atoms have been saturated with hydrogen atoms to reduce boundary effects. It should be mentioned that structural, mechanical, electronic and magnetic properties of finite size graphene may depend on the edge atoms. Further experimental probes have revealed intriguing preference of a particular edge type (zigzag vs. armchair). But it has no significant influence on the results of our work.

These effects can be ignored when the results of gas molecules adsorbed on the graphene surface are compared based on the same system and calculation method. Obtaining absolute values for different parameters of the systems is not our concern, while we want to study the change of different characters upon adsorption processes.

Geometry optimizations, energy calculations, and density of states (DOS) analysis have been performed on graphene and different CO/graphene complexes using B3LYP functional with 6–31G(d) basis set as implemented in GAMESS suite of program [22]. GaussSum program has been used to obtain DOS results [23]. The B3LYP is demonstrated to be a reliable and commonly used functional in the study of different nanostructures [24–27]. We have defined adsorption energy in the usual way as:

$$E_{\text{ad}} = E(\text{CO/graphene}) - E(\text{graphene}) - E(\text{CO}) + E_{\text{BSSE}}, \quad (1)$$

where $E(\text{CO/graphene})$ corresponds to the energy of the CO/graphene in which the CO has been adsorbed on the surface, $E(\text{graphene})$ is the energy of the isolated sheet, $E(\text{CO})$ is the energy of a single CO molecule, and E_{BSSE} is the energy of the basis set superposition error. By definition, a negative value of E_{ad} corresponds to exothermic adsorption. The canonical assumption for Fermi level is that in a molecule (at $T = 0 \text{ K}$) it lies approximately in the middle of the

Table 1 Adsorption energy (E_{ad} in kcal mol^{-1}), HOMO energies (E_{HOMO}), LUMO energies (E_{LUMO}) and HOMO-LUMO energy gap of pristine systems in eV at B3LYP level of theory

Configuration	E_{ad}	${}^{\text{a}}Q_{\text{T}}$ (e)	E_{HOMO}	E_{LUMO}	E_{g}	${}^{\text{b}}\Delta E_{\text{g}}$ (%)
graphene	–	–	–3.73	–3.48	0.25	–
(a) CO/graphene	–0.56	–0.003	–3.72	–3.48	0.24	–4.0
(b) CO/graphene	–0.44	–0.001	–3.73	–3.48	0.25	0.0
(c) CO/graphene	–0.37	0.000	–3.72	–3.46	0.26	+4.0
(d) CO/graphene	–0.28	0.000	–3.72	–3.47	0.25	0.0
(e) CO/graphene	–0.20	0.000	–3.72	–3.48	0.24	–4.0
(f) CO/graphene	–0.15	0.000	–3.71	–3.47	0.24	–4.0

${}^{\text{a}}Q_{\text{T}}$ is defined as the total Mulliken charge on the molecule

${}^{\text{b}}\Delta E_{\text{g}}$ Change of E_{g} of pristine graphene after CO adsorption

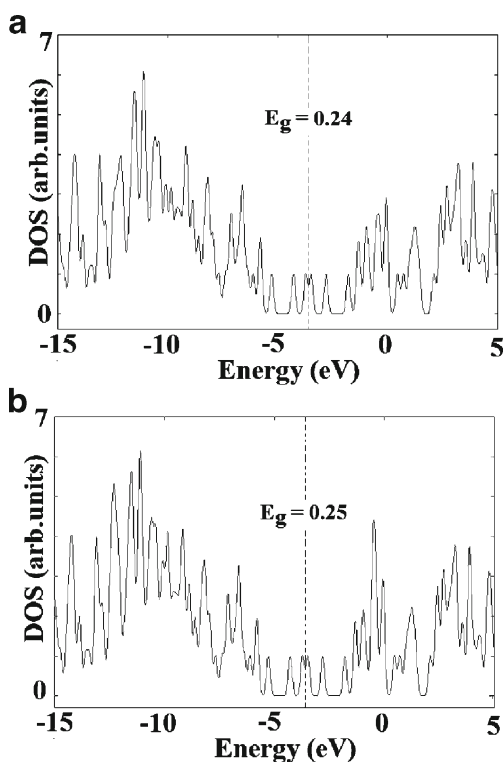


Fig. 2 Comparison of density of states (DOS) of P-graphene and CO/P-graphene

highest occupied molecular orbital (HOMO) and the lowest unoccupied molecular orbital (LUMO) energy gap (E_g). In fact, what lies in the middle of the E_g is the chemical potential, and since the chemical potential of a free gas of

electrons is equal to its Fermi level as traditionally defined, herein, the Fermi level of the considered systems is at the center of the E_g .

Results and discussion

The pristine graphene

At first, we investigated the most stable configuration of CO adsorbed on the P-graphene. Several initial configurations have been considered in order to study the adsorption of CO on the P-graphene. A CO molecule was initially placed above a carbon atom or the center of a six-membered ring (6MR), with the CO molecule oriented perpendicular (with the C or O atom pointing toward the graphene sheet) to the graphene. Several other configurations with the CO molecule, which were placed parallel to the graphene plane, were also tested. After full relaxation, a configuration with the adsorbed CO axis aligned parallel to the graphene plane along the axis of two opposite C atoms of the 6MR was found to be the most stable one for the P-graphene. The E_{ad} of this system is $-0.56 \text{ kcal mol}^{-1}$ and the molecule-sheet distance is 4.22 \AA (Fig. 1a). The low E_{ad} and long distance indicate a weak interaction.

The charge transfer between CO and P-graphene was obtained from Mulliken population analysis (Table 1). For CO on P-graphene, the calculated charges on the C and O atoms of the CO are about 0.180 and $-0.183 e$, respectively, while there was no charge on the C atoms of the P-graphene.

Fig. 3 Structure of optimized (a) SW-graphene, (b) CO/SW-graphene complex and their density of states (DOS). Bonds are in \AA

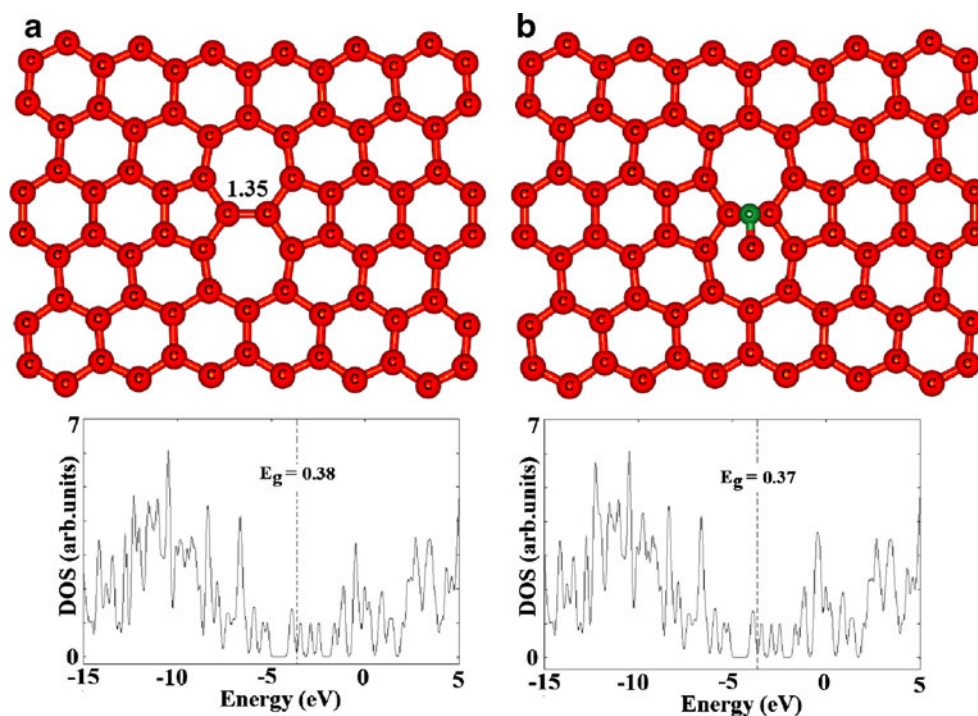


Table 2 Adsorption energy (E_{ad} in kcal mol^{-1}), HOMO energies (E_{HOMO}), LUMO energies (E_{LUMO}) and HOMO-LUMO energy gap (E_{g}) of modified systems in eV at B3LYP level of theory

Configuration	E_{ad}	${}^{\text{a}}Q_{\text{T}}$ ($ e $)	E_{HOMO}	E_{LUMO}	E_{g}	${}^{\text{b}}\Delta E_{\text{g}}$ (%)
SW-graphene	–	–	–3.83	–3.45	0.38	–
CO/SW-graphene	–1.01	–0.008	–3.83	–3.46	0.37	–2.6
Si-graphene	–	–	–3.77	–3.51	0.26	–
S.1	–4.77	0.014	–3.71	–3.46	0.25	–3.8
S.2	–11.40	0.029	–3.71	–3.45	0.26	0.0
Al-graphene	–	–	–3.99	–3.67	0.32	–
A.1	–13.75	0.201	–3.79	–3.52	0.27	–15.6
A.2	–11.61	0.139	–4.17	–2.98	1.19	+272.0

${}^{\text{a}}Q_{\text{T}}$ is defined as the total Mulliken charge on the molecule

${}^{\text{b}}\Delta E_{\text{g}}$ Change of E_{g} of modified graphene after CO adsorption

Meanwhile, a very small charge ($0.003 e$) is transferred from the P-graphene to CO. This is in quite good agreement with Zhang's results [21]. To verify the effects of the adsorption of CO on the P-graphene electronic properties, the DOS plots of CO/P-graphene adsorption systems were calculated and Fig. 2 shows the DOS for some representative systems. The results suggest that the CO molecule weakly interacts with P-graphene. Also, the DOS of the P-graphene (Fig. 2a) is similar to that of the most stable CO/P-graphene (Fig. 2b). The contribution of the CO electronic levels to the DOS for all systems is far away from the Fermi level.

Stone-Wales defected graphene

The SW defect is created by rotating a carbon dimer 90° and the relaxed geometry of graphene with Stone-Wales defect (SW-graphene) and it is shown in Fig. 3a. The main change in the atomic structure is that the C-C bond belonging to the defect is compressed and stretched. Especially, the rotated bond is changed from a perfect state 1.43 to 1.35 Å. In the stable SW-graphene structure, defect atoms move out of plane in the opposite direction in order to lower the energy by allowing the compressed C-C bonds in its vicinity to expand. Similarly, the CO molecule was initially placed

on the various sites of the SW-graphene with different orientations to find the optimal adsorption configurations. However, only one local minimum structure was obtained upon the relaxation process. The value of E_{ad} for SW-graphene complex (Fig. 3b) is about $-1.01 \text{ kcal mol}^{-1}$ which is larger than the E_{ad} of CO/P-graphene complex. This indicates that the existence of SW defect increases the reactivity of graphene toward the adsorption of CO molecule.

Adsorption of CO molecule did not introduce a serious structural distortion. The binding distance, which is defined as the length between the O atom of CO molecule and the center of defected C-C bond in graphene, is 3.51 Å and is lower than that of CO/P-graphene complex. More detailed information about the simulation of the different CO/modified graphene systems is listed in Table 2. The low negative E_{ad} and large binding distance imply that CO molecule floats above the sheet, and there is no evidence to indicate that a chemical bond is formed between the CO molecule and the SW-graphene. Such weak interaction between the CO molecule and the SW-graphene is a characteristic property of physisorption similar to that of CO/P-graphene complex.

By comparing the DOS curve of the SW-graphene with that of the CO/SW-graphene complex depicted in Fig. 3, it

Fig. 4 Structure of optimized (a) Si-graphene, (b) Al-graphene and their density of states (DOS). Bonds are in Å

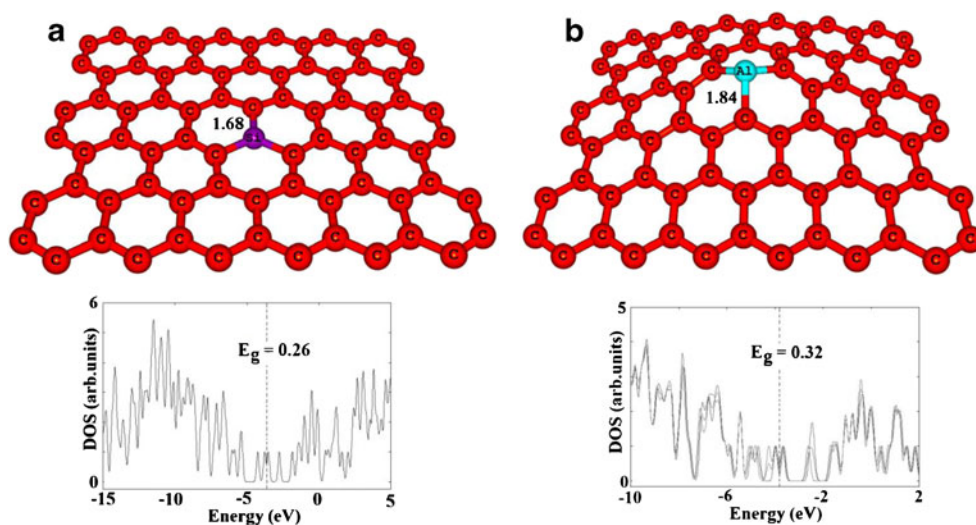
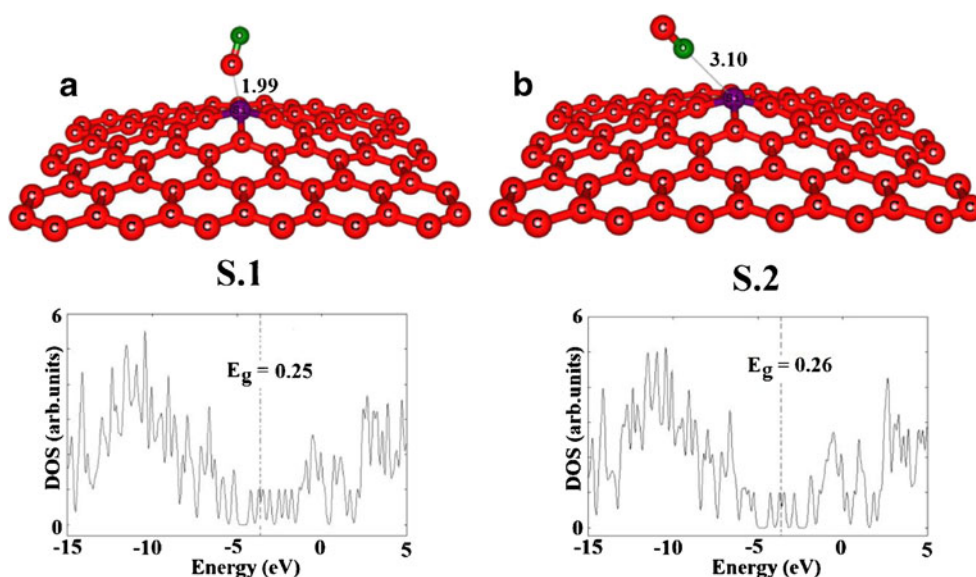


Fig. 5 Optimized structures of CO/Si-graphene complexes and their density of states (DOS). Bonds are in Å



becomes clear that after the CO adsorption, a distinct change is not observed in the E_g of the sheet. The computed E_g of the SW-graphene and CO/SW-graphene complex is about 0.38 and 0.37 eV, respectively. The charge transferred between CO and SW-graphene is very small (0.008 e), confirming the insignificant change of E_g of SW-graphene. The SW-graphene is, therefore, not sensitive to the presence of CO molecules. To overcome this weakness of pristine and SW-defected graphene, we proposed to modify the electrical and chemical properties of pristine sheet through doping impurity atoms on P-graphene. Thus, we replaced one carbon atom of P-graphene surface by silicon and aluminum atoms.

Silicon doping

We have observed that the silicon atom projects out of the sheet and creates local deformation due to its larger covalent

radius (1.11 Å) compared with carbon atom (0.77 Å). The deformation at silicon site shows all Si–C bonds are of 1.67 Å and they are larger than C–C bonds (1.43 Å) (Fig. 4a). However, the planarity of the sheet is not affected by Si-doping and hybridization of Si remained sp^2 similar to C atom. Further, Mulliken population analysis shows that silicon atom acquires positive charge of magnitude 0.238 e . This shows that the charge is transferred from the silicon atom to the vicinity carbon atoms. Such charge polarization at dopant site (silicon atom) acts as an affinity center for chemisorption of the CO molecules.

We have performed calculations to observe the interaction of CO on Si-graphene and traced the most stable configurations. However, only two local minima were obtained upon the relaxation process (Fig. 5). Configuration S.1 stands for a weak van der Waals interaction between CO molecule and the sheet. In this configuration, CO molecule

Fig. 6 Optimized structures of CO/Al-graphene complexes and their density of states (DOS). Bonds are in Å

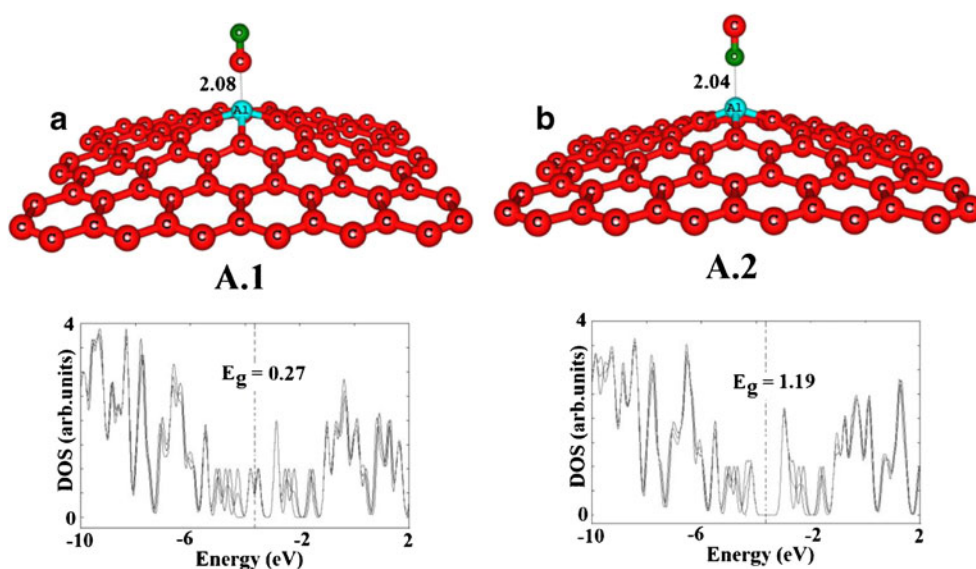


Table 3 Adsorption energy (E_{ad} in kcal mol⁻¹), HOMO energies (E_{HOMO}), LUMO energies (E_{LUMO}) and HOMO-LUMO energy gap of pristine systems in eV at B97D level of theory^a Q_{T} is defined as the total Mulliken charge on the molecule^bChange of E_{g} of pristine graphene after CO adsorption

Configuration	E_{ad}	^a Q_{T} (e)	E_{HOMO}	E_{LUMO}	E_{g}	^b ΔE_{g} (%)
graphene	–	–	–3.64	–3.53	0.11	–
(a) CO/graphene	–1.67	–0.004	–3.68	–3.60	0.10	–9.1
(b) CO/graphene	–1.51	–0.002	–3.67	–3.74	0.11	0.0
(c) CO/graphene	–1.31	0.000	–3.75	–3.84	0.10	–9.1
(d) CO/graphene	–1.16	0.000	–3.63	–3.52	0.11	–0.0
(e) CO/graphene	–1.02	0.001	–3.69	–3.79	0.10	–9.1
(f) CO/graphene	–0.79	0.000	–3.78	–3.65	0.10	–9.1

from its carbon atom was located atop of Si atom and its corresponding calculated E_{ad} value (Table 2) is about -4.77 kcal mol⁻¹. As shown in Fig. 5b, the most stable configuration of the CO/Si-graphene system (**S.2**) is that in which the O atom of CO is close to Si atom with equilibrium distance of 3.10 Å. As shown in Table 2, the adsorption behavior of CO is significantly different from that on the P-graphene. The calculated E_{ad} in configuration **S.2** is -11.40 kcal mol⁻¹, which is larger by 10.84 kcal mol⁻¹ than that of CO interacting with P-graphene. It indicates that the interaction of CO with Si-graphene is much stronger than that with the pristine graphene. Its E_{ad} value is also more negative than E_{ad} between CO and SW-graphene.

It has also been found that the Si-graphene undergoes an obvious distortion upon CO adsorption (Fig. 5b), so based on the NBO analysis, the adsorbing Si atom is transformed from sp^2 hybridization to sp^3 . Calculated DOS of Si-graphene is shown in Fig. 4a, indicating that its E_{g} value is slightly increased to 0.26 eV compared to the P-graphene. However, the CO adsorption on this doped-system has insignificant effect on the E_{g} values of Si-graphene (Table 2). The computed ΔE_{g} percentage for configurations **S.1** and **S.2** is 3.8 % or 0.0 %, indicating that substitution of C by Si atom cannot notably change the sensitivity of the sheet.

Aluminum doping

When the carbon atom was replaced by an Al atom, the structure around the adsorbed site was significantly changed.

As it is known, an Al atom has one less valence electron than a C atom and its doping processes yield a *p*-type semiconductor. As shown by panel b in Fig. 4, the geometric structure of P-graphene was dramatically distorted, where the impurity Al projects out of the sheet due to its larger size than C atom. The calculated bond lengths are 1.84 Å for the neighboring Al-C bond in the doped sheet which is much longer than the corresponding C-C bonds in the pure sheet. Also, the C–Al–C angle in the doped sheet is 114° which is smaller than C–C–C in the pristine sheet (120°), which the NBO analysis suggests can be attributed to the change of doped site hybridization from sp^2 to nearly sp^3 . Subsequently, we have explored CO adsorption on the Al-graphene by locating the molecule above the Al atom with different initial orientations including O or C atom of the molecule being close to Al.

After careful relaxed optimization of initial structures similar to Si-graphene sheet, two final stable structures were obtained. The most and second most stable adsorption structures are shown in Fig. 6, where the C and O atom of CO is close to Al atom of the sheet (namely **A.1** and **A.2** configurations, respectively). As shown in Table 2, the adsorption behavior of CO is significantly different from that on the Si-graphene. The calculated adsorption energy of CO from C head (as most stable configuration (**A.1**)) is -13.75 kcal mol⁻¹, which is more exothermic by 2.35 kcal mol⁻¹ than that of CO interacting from its O head with Si-graphene (as most stable configuration (**S.2**)). Since Al has one electron less than carbon, the Al-graphene is an electron-deficient system. When the CO atoms are adsorbed on the Al-

Table 4 Adsorption energy (E_{ad} in kcal mol⁻¹), HOMO energies (E_{HOMO}), LUMO energies (E_{LUMO}) and HOMO-LUMO energy gap (E_{g}) of modified systems in eV at B97D level of theory^a Q_{T} is defined as the total Mulliken charge on the molecule^bChange of E_{g} of modified graphene after CO adsorption

Configuration	E_{ad}	^a Q_{T} (e)	E_{HOMO}	E_{LUMO}	E_{g}	^b ΔE_{g} (%)
SW-graphene	–	–	–3.43	–3.39	0.04	–
CO/SW-graphene	–7.38	–0.011	–3.32	–3.28	0.04	0.0
Si-graphene	–	–	–3.66	–3.64	0.03	–
S.1	–11.30	0.034	–3.52	–3.51	0.01	–33.3
S.2	–14.28	0.030	–3.71	–3.69	0.02	0.0
Al-graphene	–	–	–3.78	–3.33	0.45	–
A.1	–26.89	0.155	–3.72	–3.48	0.24	–46.6
A.2	–19.65	0.104	–3.81	–2.67	1.14	+153.3

graphene, there will be large electron transfer from the CO molecule to the Al-graphene, which makes the CO molecule more strongly bound than Al-graphene.

Furthermore, for investigating the change of electronic structures in modified graphene caused by the adsorption of CO molecule, the net charge transfer (Q) between the sheet and molecule is calculated by Mulliken analysis. $Q=0.029 e$ in the CO/Si-graphene complex and is larger than $Q=0.008 e$ in the CO/SW-graphene complex. The result reveals that the Si doping leads to a relatively strong binding interaction between the CO molecule and the graphene surface. As listed in Table 2, $Q=0.201 e$ in the CO/Al-graphene complex is one order larger than $0.029 e$ in the CO/Si-graphene complex, which is in accordance with their E_{ad} .

Calculated DOS of Al-graphene is shown in Fig. 4b, indicating that its E_g value is reduced to 0.32 eV compared to the P-graphene. It should be noted that, herein, the E_g also stands for singly occupied molecular orbital (SOMO)/LUMO energy gaps for the open shell systems. After CO adsorption in configuration A.2 valence level shifted to higher energies (−2.98 eV) compared to the bare Al-graphene (−3.67 eV) so, the E_g of sheet increased from 0.32 to 1.19 eV (Fig. 6b). It is well known that the E_g (or band gap in bulk materials) is a major factor determining the electrical conductivity of a material and there is a classic relation between them as follows [28]

$$\sigma \propto \exp\left(\frac{-E_g}{2kT}\right), \quad (2)$$

where σ is the electrical conductivity and k is the Boltzmann's constant. According to the equation, larger E_g at a given temperature leads to smaller electrical conductivity. The considerable change of about 272 % (Table 2) in the E_g value demonstrates the high sensitivity of the electronic properties of Al-doped graphene toward the CO adsorption on its surface. To summarize, we have demonstrated that the tunable E_g of up to ≈ 1.19 eV can be engineered in graphene by the controlled adsorption of CO molecule to the surface of Al-doped graphene.

Finally, we have explored the effect of method on the obtained results. The dispersion term to the total energy may give a non-negligible contribution, especially in the calculation of the physisorption processes. Therefore, we have repeated all of the energy calculations, using semiempirically dispersion corrected functional B97D [29] with the same basis set. The results have been summarized in Tables 3 and 4, showing that the E_{ad} values of B97D are somewhat more negative than those of the B3LYP, especially in the cases of CO adsorption on the pristine graphene. It may be due to the fact that the B97D includes dispersion interactions. Interestingly, it was found that the E_g values strongly depend on the type of functional method. As seen in Table 3, the B97D

significantly underestimates the E_g value (in comparison with B3LYP) so that that it is about 0.11 eV for pristine graphene which is noticeably lower than the value of B3LYP. However, the results of B97D also confirms the main finding of this research that the tunable E_g of up to ≈ 1.14 eV (Table 4) can be engineered in graphene by the controlled adsorption of CO molecule to the surface of Al-doped graphene.

Conclusions

Adsorption of CO molecule on the pristine, SW-defected Al- and Si- doped graphenes was investigated using DFT calculations. It is found that CO molecule is weakly adsorbed on the P- and SW-graphenes with large separation. The electronic properties of the P- and SW-graphenes were slightly changed upon the adsorption of CO molecule. In contrast, the CO molecule shows strong interactions with the Al- and Si- doped graphenes. The significantly increased thermodynamic favorability and charge transfer of CO on the Al-graphene are expected to induce significant changes in the electrical conductivity of the sheet. Here, we demonstrate the existence of a large E_g opening of 0.87 eV in graphene, induced by Al-doping and CO adsorption.

References

1. Tontapha S, Ruangpornvisuti V, Wannoo B (2012) J Mol Model doi:10.1007/s00894-012-1537-6
2. Tadeev AV, Delabouglise G, Labeau M (1999) Thin Solid Films 337:163–165
3. Peyghan AA, Baei MT, Hashemian S, Torabi P (2013) J Mol Model 19:859–870
4. Joshi RK, Hu Q, Alvi F, Joshi N, Kumar A (2009) J Phys Chem C 113:16199–16202
5. Beheshtian J, Bagheri Z, Kamfiroozi M, Ahmadi A (2011) Microelectron J 42:1400–1403
6. Beheshtian J, Bagheri Z, Kamfiroozi M, Ahmadi A (2012) Struct Chem 23:653–657
7. Rastegar SF, Peyghan AA, Hadipour NL (2012) Appl Surf Sci 265:412–417
8. Novoselov KS, Geim AK, Morozov SV, Jiang D, Zhang Y, Dubonos SV, Grigorieva IV, Firsov AA (2004) Science 306:666–669
9. Beheshtian J, Soleymanabadi H, Peyghan AA, Bagheri Z (2012) Appl Surf Sci 268:436–441
10. Contreras CN, Cocolletzi HH, Anoto EC (2011) J Mol Model 17:2093–2097
11. Chen Y, Gao B, Zhao JX, Cai QH, Fu HG (2012) J Mol Model 18:2043–2054
12. Schedin F, Geim AK, Morozov SV, Hill EW, Blake P, Katsnelson MI, Novoselov KS (2007) Nat Mater 6:652–655
13. Nomani MWK, Shishir R, Qazi M, Diwan D, Koley G, Shields VB, Spencer MG, Tompa GS, Sbrockey NM (2010) Sensor Actuat B Chem 150:301–307
14. Romero HE, Joshi P, Gupta AK, Gutierrez HR, Cole MW, Tadigadapa SA, Eklund PC (2009) Nanotechnology 20: 245501–245508
15. Katsnelson MI, Novoselov KS, Geim AK (2006) Nat Phys 2:620–625

16. Guinea F, Katsnelson MI, Geim AK (2010) *Nat Phys* 6:30–33
17. Balog R, Jorgensen B, Nilsson L, Andersen M, Rienks E, Bianchi M, Fanetti M, Laegsgaard E, Baraldi A, Lizzit S, Sljivancanin Z, Besenbacher F, Hammer B, Pedersen TG, Hofmann P, Hornekaer L (2010) *Nat Mater* 9:315–319
18. Meyer JC, Girit CO, Crommie MF, Zettl A (2008) *Appl Phys Lett* 92:123110–123113
19. Son YW, Cohen ML, Louie SG (2006) *Phys Rev Lett* 97:216803–216806
20. Pedersen TG, Flindt C, Pedersen J, Mortensen NA, Jauho AP, Pedersen K (2008) *Phys Rev Lett* 100:136804–136807
21. Zhang YH, Chen YB, Zhou KG, Liu CH, Zeng J, Zhang HL, Peng Y (2009) *Nanotechnology* 20:185504–185511
22. Schmidt MW, Baldrige KK, Boatz JA, Elbert ST, Gordon MS, Jensen JH, Koseki S, Matsunaga N, Nguyen KA, Su S, Windus TL, Dupuis M, Montgomery JA (1993) *J Comput Chem* 14:1347–1363
23. O'Boyle N, Tenderholt A, Langner K (2008) *J Comput Chem* 29:839–845
24. Beheshtian J, Bagheri Z, Kamfiroozi M, Ahmadi A (2012) *J Mol Model* 18:2653–2658
25. Beheshtian J, Kamfiroozi M, Bagheri Z, Peyghan AA (2012) *Chin J Chem Phys* 25:60–64
26. Beheshtian J, Peyghan AA, Bagheri Z (2012) *Comput Mater Sci* 62:71–74
27. Moradi M, Peyghan AA, Bagheri Z, Kamfiroozi M (2012) *J Mol Model* 18:3535–3540
28. Li S (2006) *Semiconductor physical electronics*, 2nd edn. Springer, Berlin
29. Grimme S (2006) *J Comput Chem* 27:1787–1799